Hydrogen Bonding Constrains Free Radical Reaction Dynamics at Serine and Threonine Residues in Peptides

ARTICLE *in* THE JOURNAL OF PHYSICAL CHEMISTRY A · MARCH 2014

Impact Factor: 2.69 · DOI: 10.1021/jp501367w · Source: PubMed

4 AUTHORS, INCLUDING:

Chang Ho Sohn
California Institute of Technology
11 PUBLICATIONS **117** CITATIONS
SEE PROFILE

Jinshan Gao
Montclair State University
6 PUBLICATIONS **32** CITATIONS
SEE PROFILE

THE JOURNAL OF PHYSICAL CHEMISTRY A

Article

pubs.acs.org/JPCA

Hydrogen Bonding Constrains Free Radical Reaction Dynamics at Serine and Threonine Residues in Peptides

Daniel A. Thomas, Chang Ho Sohn, Jinshan Gao, and J. L. Beauchamp*

Arthur Amos Noyes Laboratory of Chemical Physics, California Institute of Technology, Pasadena, California 91125, United States

Supporting Information

ABSTRACT: Free radical-initiated peptide sequencing (FRIPS) mass spectrometry derives advantage from the introduction of highly selective low-energy dissociation pathways in target peptides. An acetyl radical, formed at the peptide N-terminus via collisional activation and subsequent dissociation of a covalently attached radical precursor, abstracts a hydrogen atom from diverse sites on the peptide, yielding sequence information through backbone cleavage as well as side-chain loss. Unique free-radical-initiated dissociation pathways observed at serine and threonine residues lead to cleavage of the neighboring N-terminal C_α–C or N–C_α bond rather than the typical C_α–C bond cleavage observed with other amino acids. These reactions were investigated by FRIPS of model peptides of the form AARAAAXAA, where X is the amino acid of interest. In combination with density functional theory (DFT) calculations, the experiments indicate the strong influence of hydrogen bonding at serine or threonine on the observed free radical chemistry. Hydrogen bonding of the side-chain hydroxyl group with a backbone carbonyl oxygen aligns the singly occupied π orbital on the β-carbon and the N–C_α bond, leading to low-barrier β-cleavage of the N–C_α bond. Interaction with the N-terminal carbonyl favors a hydrogen-atom transfer process to yield stable c and z$^\bullet$ ions, whereas C-terminal interaction leads to effective cleavage of the C_α–C bond through rapid loss of isocyanic acid. Dissociation of the C_α–C bond may also occur via water loss followed by β-cleavage from a nitrogen-centered radical. These competitive dissociation pathways from a single residue illustrate the sensitivity of gas-phase free radical chemistry to subtle factors such as hydrogen bonding that affect the potential energy surface for these low-barrier processes.

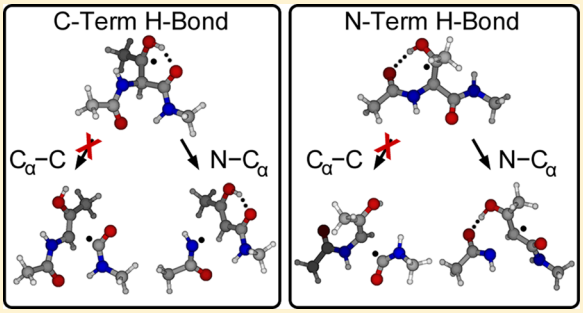

INTRODUCTION

Over the last two decades, the use of mass spectrometry experiments for the sequencing of biological molecules has been a major field of research, especially in the area of protein analysis, where high resolution and unparalleled sensitivity make tandem mass spectrometry (MS/MS) experiments the method of choice.[1−5] Successful dissociation of peptides or proteins in the gas phase is essential for obtaining peptide sequence information, and collision-induced dissociation (CID) and infrared multiphoton dissociation (IRMPD) remain the most widely utilized approaches for inducing backbone cleavage even after several decades of research.[6−9] In these techniques, input energy is statistically redistributed throughout the degrees of freedom of the peptide, resulting predominantly in the cleavage of the amide linkage and generally yielding significant sequence coverage.[10] However, shortcomings of these methods become apparent in the examination of peptides containing aspartic and glutamic acid or proline residues, where cleavage is highly selective, as well as in the analysis of post-translational modifications (PTMs), which are typically lost as neutral fragments in low-energy pathways.[9,11]

Partially in response to these limitations, the past decade has seen the development of new techniques that rely on radical-induced dissociation to provide sequence information. These methods can generally be grouped by their utilization of either hydrogen-abundant or hydrogen-deficient radicals.[12] Hydrogen-abundant radical techniques include electron capture and electron transfer dissociation (ECD and ETD, respectively), which mainly effect cleavage of backbone N–C_α bonds through the capture of low-energy electrons, yielding N-terminal c and C-terminal z$^\bullet$ products.[8,13−15] The unexpected cleavage of the comparatively strong N–C_α bond has led to a large body of work investigating the mechanism of ETD and ECD,[13,16−22] with the Utah–Washington (UW) mechanism proposed independently by Simons and co-workers[23−31] and Tureček and co-workers[21,32−38] being the most prevalent explanation. This mechanism posits that N–C_α bond dissociation occurs by electron attachment to an amide π^* orbital, either by direct electron capture or by intramolecular transfer from a high n-Rydberg state, yielding an amide radical "superbase" anion, which rapidly undergoes N–C_α bond cleavage.[19,33] Though significant progress has been achieved in elucidating the mechanism of ECD and ETD, many questions about this

Special Issue: A. W. Castleman, Jr. Festschrift

Received: February 7, 2014
Revised: March 3, 2014
Published: March 7, 2014

dx.doi.org/10.1021/jp501367w | J. Phys. Chem. A 2014, 118, 8380−8392

intriguing process remain under debate, such as the initial site of electron capture or transfer and the order of N−C_α bond cleavage and proton transfer.[19,39−41] The success of these techniques, however, is not disputed; they provide extensive sequence coverage through predominantly nonselective backbone cleavage with retention of PTMs.[9,42−44] These attributes, along with the ability to selectively cleave disulfide bonds, make ECD and ETD excellent methods for a wide range of proteomic analyses, from identification of glycosylation sites to the analysis of disulfide linkages.[4,9,16,17,45,46]

Parallel to the development and implementation of the hypervalent radical techniques, many research groups investigated methods for the formation of hydrogen-deficient radical peptides. Initially, these species were generated by UV photoionization of aromatic residues or CID of copper coordination complexes to generate copper-bound peptide radicals.[47] More recent work has established simple techniques for the generation of hydrogen-deficient peptide radicals, including CID of an array of peptide−metal complexes,[48−54] peptide irradiation with 157 nm light,[55−57] and photodissociation of carbon−iodine bonds.[58−60] To achieve regioselective free radical generation via collisional activation, Porter and co-workers converted the lysine side chain to a peroxycarbamate moiety,[61,62] whereas O'Hair and co-workers utilized nitrosylation and nitrate ester formation at cysteine and serine residues, respectively.[63−67] In addition, Hodyss and co-workers developed the technique of free-radical-initiated peptide sequencing (FRIPS), in which a well-defined radical site is produced at the N-terminus of a peptide or protein by dissociation of a covalently bound free radical precursor through a low-energy pathway.[68] The initial free radical precursor developed for this experiment was based on the Vazo-68 free radical initiator, which was coupled to the N-terminus via an acetyl group. As shown on the left side of Scheme 1, a two-step gas-phase collisional activation resulted in the generation of an acetyl radical at the N-terminus of the peptide. Later work by Lee and co-workers as well as Sohn and co-workers employed processes involving the use of the stable TEMPO (2,2,6,6-tetramethylpiperidine-1-oxyl) free radical,[69−72] which provides the advantage of requiring only a single stage of collisional activation for radical generation, as demonstrated on the right side of Scheme 1. The latter methodology is employed in the current investigation.

Unlike ECD and ETD, FRIPS and other hydrogen-deficient radical techniques produce primarily cleavage of C_α−C bonds and side-chain losses.[68,73,74] These products are formed by the abstraction of a hydrogen atom by the initial radical center from the backbone C_α or the side-chain C_β or C_γ position of a given amino acid residue followed by β-cleavage. As outlined in Scheme 2, the site of hydrogen atom abstraction generally determines the types of product ions formed. Hydrogen abstraction from C_α results in the loss of an odd-electron side-chain fragment through β-cleavage of the C_β−C_γ bond (Scheme 2a). The loss of an even-electron side-chain fragment results from C_γ−H abstraction through a similar process, giving a radical peptide ion (Scheme 2c). Backbone cleavage occurs following hydrogen abstraction from C_β, except at methionine residues, where the loss of a sulfhydryl radical is favored (Scheme 2b). This process is highly sensitive to amino acid side-chain chemistry, owing to subtle differences in dissociation energetics that modulate which product is favored. A study by Julian and co-workers using a noncovalently associated 18-crown-6 free radical precursor concluded that the amino acids

Scheme 1. Generation of Peptide Free Radicals by N-Terminal Derivatization and Gas-Phase Collisional Activation

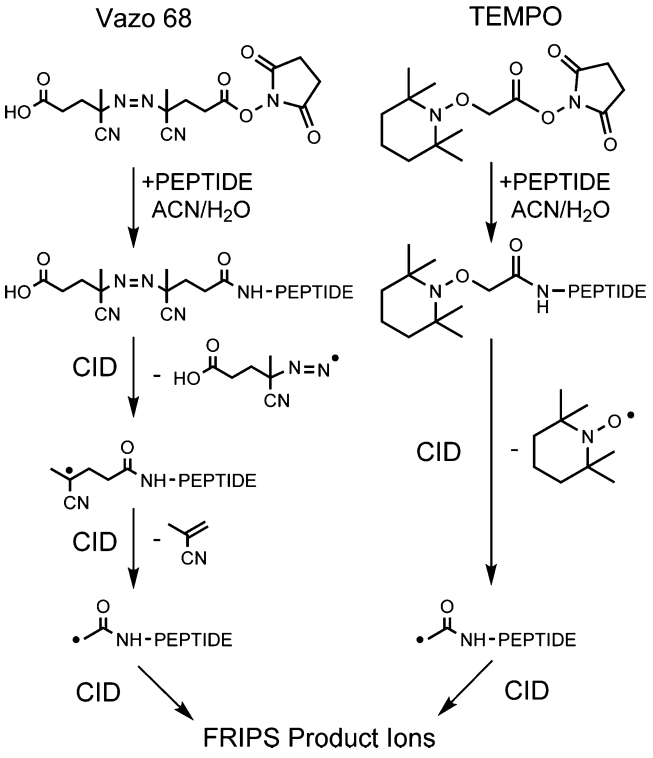

Scheme 2. Mechanism of Peptide Dissociation by Hydrogen-Deficient Free Radical Chemistry

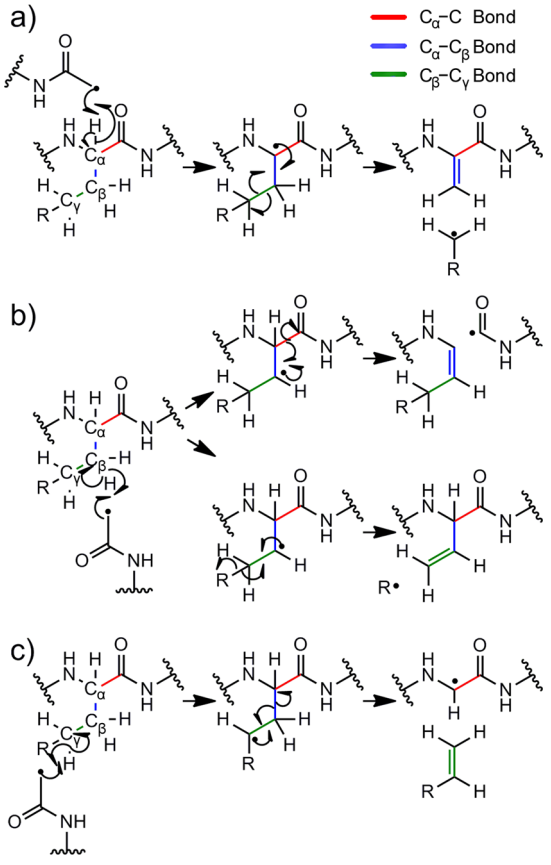

dx.doi.org/10.1021/jp501367w | J. Phys. Chem. A 2014, 118, 8380−8392

generally fall into three main categories: (1) nonreactive residues (Ala, Gly, Pro), (2) backbone C_α–C bond cleavage residues (Asp, Asn, His, Tyr, Phe, Val, Trp), and (3) side-chain loss residues (Lys, Glu, Gln, Arg, Met, Cys, Ile, Leu).[75] The amino acid residues that primarily undergo side-chain loss or are largely unreactive tend to possess high bond dissociation energies (BDEs) for the C_β–H bond, whereas those that yield backbone C_α–C bond cleavage have comparable BDEs for the C_α–H and C_β–H bonds. This process is largely independent of the charge state of the precursor ion, as evidenced by the generation of similar product ions from either cations or anions,[75,76] suggesting that barriers for these processes are typically lower than those facilitated by a mobile proton to yield b- and y-type ions. In addition, there is evidence that C_β–H BDEs are not always sufficient to predict the observed product ions, as the initial radical position and the peptide or protein conformation can strongly influence observed dissociation pathways. For example, product ions are often formed at residues in close physical proximity to the site of radical formation in the low-energy peptide or protein conformations.[51,58,60,77,78] Alternately, the radical site may migrate multiple times (i.e., participate in several C–H abstraction processes) before achieving a configuration with a low barrier to bond cleavage.[70,79,80] These studies indicate that the relative importance of competitive dissociation pathways are highly dependent on subtle factors that introduce small differences in activation energies.

The unique properties of hydrogen-deficient free radical chemistry have been shown to be especially useful for a wide range of specialized proteomics experiments, including the elucidation of phosphorylation sites,[81] the analysis of cysteine residues and disulfide linkages,[70,71,82] and the detection of D-amino acids.[83] The discovery of even more innovative applications of this technique is contingent upon a comprehensive knowledge of the underlying free radical reaction dynamics. To this end, the present study investigates the atypical dissociation pathways observed at serine and threonine residues in peptides. As reported by Julian and co-workers and Reilly and co-workers,[75,84] activation of hydrogen-deficient radical ions containing serine or threonine at the *n*th residue from the N-terminus and *m*th residue from the C-terminus results in the formation of $[a_{n-1} + H]^\bullet$ and z_m ions, as well as c_{n-1} and $[z_m - H]^\bullet$ ions. However, no compelling rationale has been proposed for the formation of these products in preference to the more commonly observed a_n and $x_{m+1}^\bullet$ ions. This work posits that the hydrogen bonding capabilities of the serine and threonine moieties lead to a number of novel dissociation pathways following hydrogen atom abstraction from either C_α or C_β. Specifically, a simple hydrogen bonding interaction alters the relative activation energies for competitive dissociation pathways by stabilizing the transition state, either by optimizing orbital overlap to yield π bond formation via N–C_α bond cleavage or through accessing a hydrogen atom transfer intermediate. The sensitivity of these low-barrier free radical dissociation pathways to alterations in the free energy landscape via noncovalent interactions is a key distinction between free-radical-initiated biomolecule dissociation and standard collisional activation methods.

METHODS

Materials. The model peptides AARAAAAAA, AARAAMAHA, AARAAASAA, AARAAATAA, AARAASATA, AATAAARAA, and AARAAAT(OMe)AA (where T(OMe) denotes a methylated threonine residue) were purchased as crude synthesis products (minimum 70% purity) from Biomer Technology (Pleasanton, CA, USA). HPLC grade methanol, acetonitrile, and water were purchased from EMD Merck (Gibbstown, NJ, USA). For desalting, 10 μL pipet ZipTips with 0.6 μL C_{18} resin were purchased from Millipore Corp (Billerica, MA, USA). All other chemicals were purchased from Sigma-Aldrich (St. Louis, MO, USA).

Synthesis of TEMPO-Based FRIPS Reagent. The TEMPO-based FRIPS reagent recently developed by Sohn and co-workers in this group, based upon the procedure outlined by Lee and co-workers,[69] was synthesized and employed for free radical generation.[70] Full synthesis details can be found in the Supporting Information to this paper (Scheme S1, Supporting Information, and associated text). Briefly, the FRIPS reagent was synthesized starting with methyl 2-bromoacetate, to which the TEMPO (2,2,6,6-tetramethylpiperidine-1-oxyl) reagent was coupled to give methyl 2-(2,2,6,6-tetramethylpiperidin-1-yloxy)acetate. This compound was then converted to 2-(2,2,6,6-tetramethylpiperidin-1-yloxy)acetic acid by stirring in 2 M potassium hydroxide in tetrahydrofuran for 24 h. The free acid was then activated by mixing with trifluoroacetic-*N*-hydroxysuccinimide ester in dry *N*,*N*-dimethylformamide for 24 h to yield 2,5-dioxopyrrolidin-1-yl 2-(2,2,6,6-tetramethylpiperidin-1-yloxy)acetate, the desired TEMPO-based FRIPS reagent.

Peptide Conjugation. Approximately 20 μg of peptide and 100 μg of the TEMPO-based FRIPS reagent were dissolved in 20 μL of a 50 mM triethylammonium bicarbonate solution (pH 8.5) in 50/50% (v/v) acetonitrile/water. The conjugation of the radical precursor to the peptide was allowed to progress for 2 h before quenching the reaction by the addition of 10 μL 25% (w/w) hydroxylamine hydrochloride in H_2O to reverse any derivatization of the hydroxyl groups. The solvent was then removed with use of a centrifugal evaporator, and the peptide was resuspended in 0.1% (v/v) trifluoroacetic acid in H_2O. The solution was desalted using Millipore C_{18} ZipTips according to the manufacturer's instructions. The 5 μL elution solvent containing approximately 5 μg of peptide was brought to a final volume of 250 μL in a 50/50/0.1% (v/v) solution of methanol/water/formic acid and was electrosprayed directly into the mass spectrometer. The acquired mass spectrum demonstrated 95% or greater derivatization of the peptide with the FRIPS reagent for all peptides examined.

Mass Spectrometry. Experiments were performed in an LCQ Deca XP quadrupole mass spectrometer (Thermo-Fisher, Waltham, MA, USA). Peptide solutions were infused directly into the electrospray source of the mass spectrometer by a syringe pump at a flow rate of 3 μL/min. An electrospray voltage of 3.5 kV, capillary voltage of 41–42 V, capillary temperature of 275 °C, and tube lens voltage of −40 to −60 V were used. Other ion optics parameters were optimized by the autotune function in the LCQ tune program for maximizing the signal intensity. The precursor isolation window for MS^n experiments was set to 3.0 m/z, and the normalized collisional energy in the LCQ tune program was varied from 26% to 30% according to residual precursor ion intensities. Spectra were recorded for 50 or 100 scans based upon signal intensity.

Computational Methods. Seven structures were chosen as simple model systems for the study of the dissociation pathways of threonine. The molecules 2-acetamido-3-hydroxy-*N*-methylbutanamide, 2-acetamido-3-methoxy-*N*-methylbutanamide, and 2-acetamido-3,*N*-methylbutanamide were utilized as models for

dx.doi.org/10.1021/jp501367w | J. Phys. Chem. A 2014, 118, 8380–8392

threonine, *O*-methylthreonine, and valine, respectively. These structures were composed of amino acids with an additional N-terminal acetyl group and C-terminal methylated amine and were employed to investigate the energetics of N−C_α and C_α−C bond cleavage with an initial radical center at C_β (Figure 3a,b,d). The threonine and *O*-methylthreonine model structures were also optimized with a radical centered at C_α to examine loss of water or methanol from the side chain (Figure 3c,e, respectively). Finally, the alanine-based structures 2-acetamidopropanimide and 2-acetamido-*N*-(prop-1-en-2-yl)-propanamide were utilized for the examination of cleavage of the C_α−C bond beginning from a nitrogen-centered radical (Figure 3f,g).

Initial geometries for each molecule were generated by MC/MM conformer search with OPLS 2005 as the force field using Macromol 8.0 as implemented in Maestro 8.0 (Schrödinger Inc., Portland, OR, USA) under the linux environment. All initial structures falling within 5 kcal/mol of the lowest-energy structure were recorded and examined. Conformation space of the radical for each system was searched by substitution of the carbon radical center with boron to simulate the trigonal bonding environment. Candidate structures from these simulations were then screened manually to avoid redundancy, and the boron atom was replaced by a carbon radical site for further optimization utilizing density functional theory (DFT) with Jaguar 7.5 (Schrödinger Inc., Portland, OR, USA) at the B3LYP/6-31+G(d) level of theory. By monitoring the occurrence of imaginary vibrational frequencies, only non-transition state structures (i.e., no imaginary vibrational frequencies) were further optimized using a higher basis set at the B3LYP/6-311++G(d,p) level.

To obtain an initial potential energy surface for each reaction, the energetics of the bond dissociation process being examined were explored by geometry optimization at fixed bond distances (i.e., relaxed coordinate scan) with a step size of 0.1 Å at the B3LYP/6-31+G(d) level of theory. After visualization in Molden,[85] transition state structures were determined by a standard transition state search at the B3LYP/6-311++G(d,p) level of theory from the highest-energy conformer found, and observation of the correct transition state was confirmed by IRC calculations. Generally, only the transition state for cleavage of the bond of interest was found, as well as the energies of the products. Small barriers due to rotations about a bond or noncovalent interactions were not investigated, except in the case where the transition state for bond cleavage was separated from the enthalpy of reaction by a noncovalent complex of the product ions.

The single point energy for each structure was also calculated using the M05-2X and M06-2X density functionals with the 6-311g++G(d,p) basis set. The two new-generation meta-hybrid functionals other than B3LYP were chosen for their ability to reliably predict the energetics of organic radical reactions, as well as their strong performance in assessing hydrogen bond interactions and dipole moments.[86−88] Thermochemical corrections (zero point energy plus thermal internal energy) were calculated with the B3LYP/6-311++G(d,p) basis set at 298 K and applied to SCF calculations from all utilized density functionals. Charges derived from the electrostatic potential and Mulliken populations were calculated for selected molecules using Jaguar, and natural atomic charges were calculated using NBO 5.0 (Theoretical Chemistry Institute, University of Wisconsin, Madison, WI) at the B3LYP/6-311g++G(d,p) level of theory. All optimizations were performed using the spin unrestricted methodology, and the spin contamination was found to be small (S^2 < 0.782). All calculations were performed using computational resources kindly provided by the Material and Process Simulation center at the Beckman Institute, Caltech.

RESULTS AND DISCUSSION

Unique Product Ions Produced at Serine and Threonine. Peptide ions derivatized by the TEMPO-based FRIPS reagent were collisionally activated to provide precursors for studies of hydrogen-deficient radical-driven dissociation. The use of the TEMPO-based reagent greatly improves the signal intensity of FRIPS spectra over the previously employed Vazo 68 FRIPS reagent by eliminating an additional stage of MS/MS experiments (Scheme 1). In all experiments presented in this work, the singly protonated peptide derivatized with the TEMPO-based reagent was isolated and subjected to CID, producing the acetyl radical peptide ion (right-hand side of Scheme 1). Further dissociation of this species by collisional activation (i.e., MS^3) produced the desired FRIPS spectrum. A more comprehensive characterization of the new-generation FRIPS reagent and its chemistry in model peptides can be found in the Supporting Information.

Parts a and b of Figure 1 show the FRIPS spectra of AARAAASAA and AARAAATAA, respectively. Contrary to the expected dissociation to yield a ions or side-chain losses typically observed in FRIPS spectra, reaction at serine or threonine generates the $[a_6 + H]^\bullet$ and c_6 ions as the dominant products, with minor formation of the a_7 ion. These atypical product ions, whose assignment was confirmed by MS^n experiments (Figure S2, Supporting Information), cannot be explained by the general mechanisms outlined in Scheme 2. Also notable is a small amount of water loss and $a_7 - H_2O$ ions, which have been observed previously in free radical reactions at serine and threonine.[84] Although the FRIPS spectra for these two model peptides are nearly identical, there is a significant difference in the abundance of CO_2 loss, which can be attributed to a difference in reactivity between serine and threonine. The FRIPS spectrum of AARAASATA shown in Figure 1e further highlights this disparity, with a significantly higher abundance of product ions from reaction at threonine than serine. These differences in reactivity were investigated using DFT calculations on model systems, and it was found that the activation energy for the rate-limiting β-cleavage reactions was systematically higher for serine than threonine due to the absence of the stabilizing methyl group on the side chain (Figure S5, Supporting Information).

To further investigate the mechanism of formation of these atypical product ions, the transposed sequence of the threonine model peptide, AATAAARAA, was examined. The FRIPS spectrum shown in Figure 1d is dominated by the formation of the z_7 ion, with the $[z_7 - H]^\bullet$ (inset), a_7 ,and $x_7 - H_2O$ ions also of notable abundance. The y_6 ion is likely formed from dissociation of the z_7 species, as this ion was prominently observed upon collisional activation of the z_7 ion (Figure S3, Supporting Information). The a_7 ion results from β-cleavage of the C_α−C bond at the arginine residue, a process that gave negligible yields of the a_3 ion in the model peptides possessing an arginine near the N-terminus. This difference can again be attributed to the somewhat regioselective nature of the FRIPS reagent (Supporting Information). Similarly, the increased abundance of CO_2 neutral loss can be attributed to the decreased accessibility of the reactive threonine residue to the

dx.doi.org/10.1021/jp501367w | J. Phys. Chem. A 2014, 118, 8380−8392

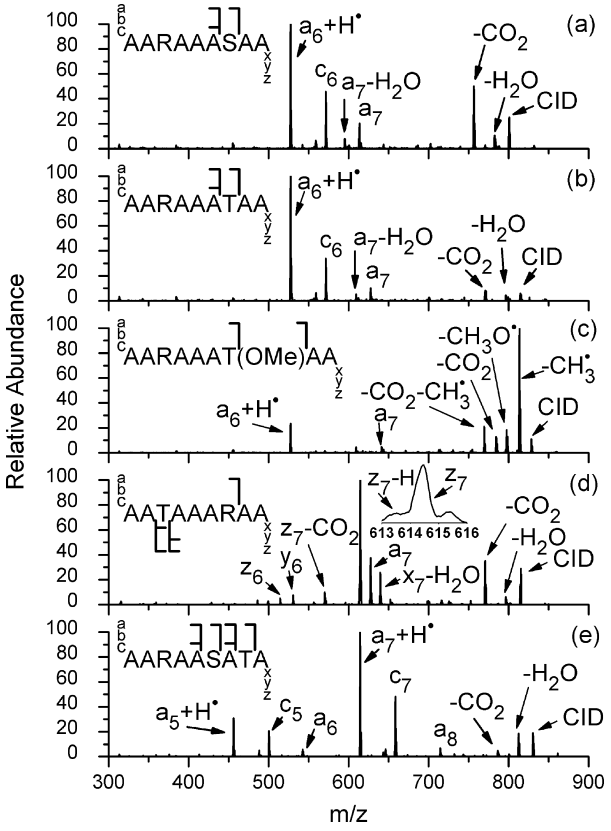

Figure 1. Free radical chemistry of serine and threonine in model peptides. For both serine (a) and threonine (b), the spectra are dominated by the formation of $[a_6 + H]^•$ and c_6 ions, instead of the more typical a_7 ion and side-chain losses. Reaction at threonine is more prominent than at serine, as seen in (e). Methylation of the hydroxyl group of threonine (c) prevents c_6 ion formation. The FRIPS spectrum of a model peptide with the threonine and arginine residues transposed to place the charge site on the C-terminal side of threonine (d) yields the z_7, $[z_7 - H]^•$, and $x_7 - H_2O$ ions.

radical site. However, given that the most prominent ions in the spectrum occur from the threonine residue near the C-terminus, the chemical properties of the various moieties on the peptide are more influential than amino acid position in determining product ion yields.

In explaining the atypical free radical chemistry of serine and threonine, attention is naturally focused on the hydroxyl group, which not only serves as a key site for modifying protein structure and function through PTMs but also has the ability to affect protein stability directly by hydrogen bonding. To determine the role this functional group plays in observed dissociation patterns, the threonine residue in the model peptide was modified by methylation of the hydroxyl group and examined using FRIPS. As shown in Figure 1c, the FRIPS spectrum is dominated by the loss of a methyl radical. This process likely occurs by hydrogen abstraction from C_β of the *O*-methylthreonine residue followed by β-cleavage of the O−CH_3 bond, resulting in the formation of a stable ketone product. Similarly, the neutral loss of the methoxy radical ($CH_3O^•$) can be explained by hydrogen abstraction from C_α of *O*-methylthreonine and subsequent β-cleavage of the C−OCH_3 bond. Interestingly, the c_6 ion is completely absent from the spectrum, implicating the necessity of the hydroxyl group for formation of this ion. In contrast, the $[a_6 + H]^•$ ion is still present, although its relative abundance is decreased, possibly due to competition with the more favorable loss of the methyl radical. The a_7 ion is similarly present with decreased relative intensity.

The presence of the $x_7 - H_2O$ ion in such great abundance in the FRIPS spectrum of AATAAARAA (Figure 1d) is rather unexpected, indicating that a favorable dissociation pathway exists for C_α−C bond cleavage coupled with water loss, likely from the threonine side chain. To further investigate the water loss pathway, MS^4 experiments were performed on the neutral loss of water from each of the model peptides, as shown in Figure 2. In each case, the spectrum predominantly consists of a

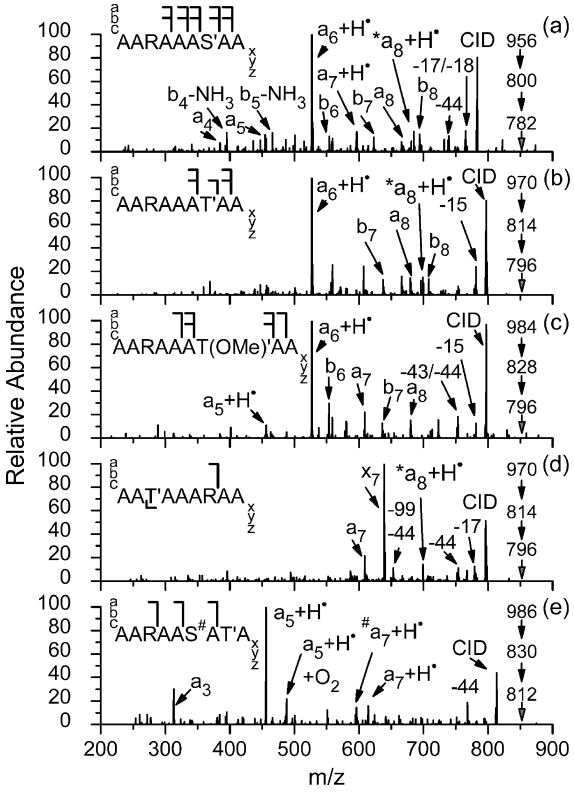

Figure 2. Collisional activation (MS^4) of the water neutral loss from model serine and threonine peptides. Each spectrum is dominated by a prominent product ion, either the $[a_{n-1} + H]^•$ ion or the x_7 ion. All product ion identifications include loss of water from serine or threonine, except those marked with *, and in (e), where # explicitly denotes water loss from serine.

single ion, either the $[a_{n-1} + H]^•$ ion when an N-terminal charge site is present or the x_m ion when there is a C-terminal charge site. Interestingly, the MS^4 spectrum of AARAASATA (Figure 2e) shows a much greater abundance of the $[a_5 + H]^•$ ion than the $[a_7 + H]^•$ ion, suggesting that the neutral loss of water occurs largely from serine rather than threonine in this case. However, whether this trend is due to peptide structural constraints or the inherent differences in the chemistry of the serine and threonine side chains is not clear from these data. Overall, these results reveal multiple reaction pathways to the $[a_{n-1} + H]^•$ ion that generate distinct C-terminal product ions, further highlighting the complex free radical chemistry of serine and threonine.

Proposed Mechanism of Reaction at Serine and Threonine Residues. It is clear from the experimental results that the common processes of C_α−C bond cleavage (from a C_β-centered radical) and side-chain loss (from a C_α-centered

dx.doi.org/10.1021/jp501367w | J. Phys. Chem. A 2014, 118, 8380−8392

Scheme 3. Proposed Mechanisms of Free-Radical-Initiated Dissociation at Serine and Threonine

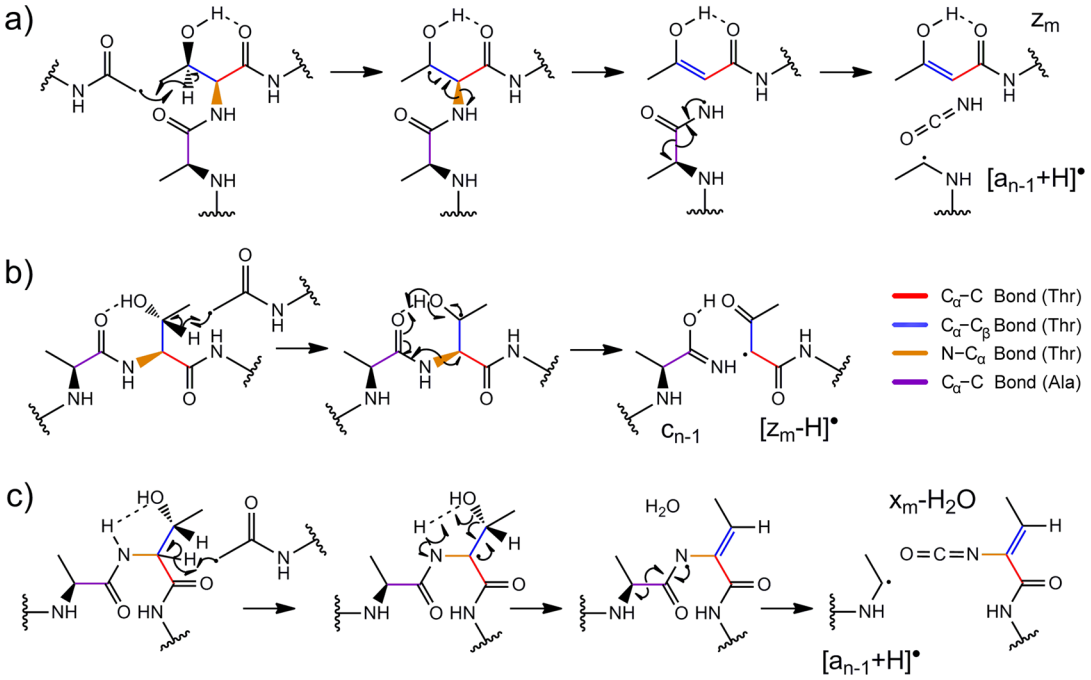

radical) are replaced by distinct lower-energy dissociation pathways at serine and threonine. Scheme 3 outlines the proposed mechanisms by which the novel product ions shown in Figure 1 are formed. All of these mechanisms posit that the presence of hydrogen bonds between the side-chain hydroxyl group and backbone amide group enables new dissociation pathways by accessing energetically favorable fragmentation processes. In spite of the relative weakness of the hydrogen bonds (~5 kcal/mol)[89−92] in comparison to the cleaved covalent bonds, these interactions are capable of significantly altering the energetic landscape by guiding access to and stabilizing transition states for otherwise noncompetitive dissociation reactions.

The $[a_{n-1} + H]^\bullet$ ion is proposed to form as a result of hydrogen bonding between the C-terminal carbonyl oxygen and the hydroxyl group, forming a six-membered ring that stabilizes the reaction intermediate, as illustrated in Scheme 3a. Due to the favorable interactions between the hydroxyl group and the carbonyl oxygen, the energy required to cleave the N−C_α bond is lowered, leading to preferential β-cleavage. This process gives the z_m ion and a $c_{n-1}^\bullet$ ion that rapidly loses isocyanic acid to give the observed $[a_{n-1} + H]^\bullet$ ion. The dominance of the $[a_{n-1} + H]^\bullet$ (Figure 1a,b) and z_m ions (Figure 1d) in the FRIPS spectra suggest that this pathway should be the most energetically favored. The hydroxyl group of serine or threonine may alternately form a seven-membered ring through hydrogen bonding with the N-terminal carbonyl oxygen atom, as shown in Scheme 3b. This conformation facilitates hydrogen atom transfer from the hydroxyl group in conjunction with hydrogen abstraction from C_β. As the N−C_α bond is elongated, the transfer of the hydrogen atom occurs in a concerted manner, reducing the reaction barrier and yielding an enol-imine c_{n-1} ion and the C_α-centered radical $[z_m - H]^\bullet$ ion. This hydrogen atom transfer process is supported by the experimental observation that methylation of the threonine hydroxyl group eliminates formation of the c_{n-1} ion. Both of these mechanisms are in agreement with those proposed by Sun et al. for the formation of c_{n-1} and radical a_{n-1} ions at serine and threonine residues through hydrogen-deficient radical dissociation from a crown ether-based photolabile radical precursor, but the importance of the hydrogen bonding interactions has not been previously demonstrated.[75]

As evidenced by the formation of $[a_{n-1} + H]^\bullet$ ions in the absence of a hydrogen bond donor (Figure 1c) as well as the formation of $[a_{n-1} + H]^\bullet$ and $x_m - H_2O$ ions following neutral loss of water (Figure 2), a third dissociation pathway must be considered at serine and threonine residues. In the mechanism shown in Scheme 3c, the hydroxyl group of serine or threonine acts as hydrogen bond acceptor instead of donor, leading to a strong interaction with the N-terminal amide hydrogen. Following hydrogen abstraction from C_α by the acetyl radical, the new radical center may undergo β-cleavage in concert with hydrogen abstraction from the backbone amide nitrogen, yielding a neutral loss of water and a nitrogen-centered radical. This nitrogen-centered radical may then undergo further β-cleavage of the N-terminal C_α−C bond to yield the observed $[a_{n-1} + H]^\bullet$ and $x_m - H_2O$ ions. A similar mechanism was previously proposed by Reilly and co-workers in their examination of the collisional activation of radical a ions produced by 157 nm photodissociation.[84] Importantly, this mechanism offers an explanation for the formation of the $[a_{n-1} + H]^\bullet$ ion even when the hydroxyl group of threonine is methylated (Figure 1c), as the methoxy group may still act as hydrogen bond acceptor and yield the nitrogen-centered radical via loss of methanol.

■ COMPUTATIONAL ANALYSIS

Given the strong experimental evidence for the mechanisms proposed in Scheme 3, in both this work and previous studies,[75,84] we investigate these reactions utilizing computational techniques to better understand the free radical chemistry of serine and threonine. The C_β-centered radical structures shown in Figure 3a,b,d were employed to examine cleavage of the N−C_α and C_α−C bond via β-cleavage, and the

dx.doi.org/10.1021/jp501367w | J. Phys. Chem. A 2014, 118, 8380−8392

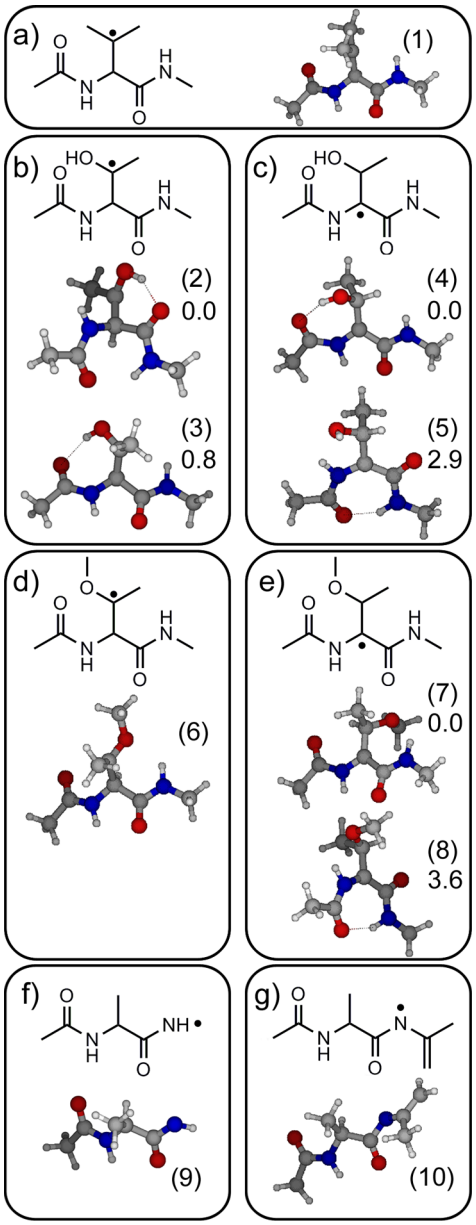

Figure 3. Model structures for computational investigation of threonine free radical chemistry. The structures of compounds possessing a C_β-centered radical are shown for valine (a), threonine (b), and *O*-methylthreonine (d), whereas those possessing a C_α-centered radical are shown for threonine (c) and *O*-methylthreonine (e). The final two compounds (f and g) were utilized to study C_α–C bond cleavage from a nitrogen-centered radical. Relative enthalpies [B3LYP/6-311++G(d,p)] are indicated for multiple structures. Hydrogen bonding interactions are denoted with dashed lines (see text for further discussion).

C_α-centered radicals in Figure 3c,e were used to explore the neutral loss of water from the side chain. Finally, the nitrogen-centered radicals shown in Figure 3f,g were used to study β-cleavage of the C_α–C bond. The structures shown beneath the schematic diagram for each molecule represent the low-energy conformer or conformers found for that compound, with the relative enthalpy (B3LYP/6-311++G(d,p) level of theory) indicated for molecules with multiple low-energy conformations of interest.

For all bond cleavage processes examined in this study, the reaction energetics were calculated using the M05-2X and M06-2X density functionals as well as B3LYP. These functionals give reaction enthalpies differing by as much as 13 kcal/mol for β-cleavage processes, with slightly smaller differences for activation energies. Previous work by Izgorodina et al. demonstrated that B3LYP may underestimate the energetics of β-cleavage reactions by up to 9 kcal/mol.[93] The M05-2X and M06-2X density functionals are expected to be significantly more accurate for these reactions, although they were found to overestimate energetics of β-cleavage by ~2 kcal/mol compared to G3(MP2)-RAD benchmarks.[88] This result can be interpreted to suggest that the computational energetics presented here likely represent bounds on the actual thermochemistry.

β-Cleavage of the N–C_α vs C_α–C Bond. To investigate the favored β-cleavage of the N–C_α bond over the C_α–C bond from a radical centered at C_β, as proposed in Scheme 3a,b, the energetics for these processes were calculated for valine, serine, and threonine model compounds (Figure 4). The energetics for the valine model compound shown in Figure 4a provide reference dissociation energetics in the absence of hydrogen bonding that might constrain the reaction intermediate to provide a low-energy pathway similar to that for serine and threonine. The low-energy conformer (**1**) has the backbone in the all-trans configuration with the side chain oriented perpendicular to the backbone. As expected, cleavage of the C_α–C bond was found to be favored over N–C_α bond cleavage by 6–10 kcal/mol depending on the density functional used, with both reactions occurring via relatively loose transition states. Dissociation of the N–C_α bond proceeds through a transition state in which a stabilizing hydrogen bond interaction between products is preserved, yielding an energetic minimum between dissociation transition state and overall reaction enthalpy of the separated products (right-hand side of Figure 4a).

Two low-energy structures were found for the threonine model compound possessing a radical center at C_β (Figure 3b), and both conformers were examined to obtain reaction energetics as shown in Figure 4b,c. These two structures possess an all-trans backbone conformation, and the side-chain hydroxyl group forms a hydrogen bond with either the C-terminal (**2**, 0.0 kcal/mol) or N-terminal (**3**, 0.8 kcal/mol) carbonyl oxygen. Although the energetics of C_α–C bond cleavage are quite similar between valine (Figure 4a) and the C-terminal hydrogen bonding structure of threonine (Figure 4b), the energy required for N–C_α bond cleavage is greatly decreased for threonine. The hydrogen bonding interactions are eliminated at the transition state for C_α–C bond cleavage (**20**) to enhance the π-orbital interactions of the N-terminal product (**22**), but the hydrogen bond persists in the transition state for N–C_α bond dissociation (**17**), reducing the energy required to form the $c^\bullet$ (**18**) and z (**19**) ion analogues of the products proposed in Scheme 3a. Similar to the case for the valine model compound, the loose transition state for N–C_α bond cleavage was found to be lower than the product enthalpies due to formation of a stabilizing hydrogen bond following dissociation. Though the B3LYP calculations clearly favor cleavage of the N–C_α bond over the C_α–C bond, the M05-2X and M06-2X calculations give similar reaction enthalpies for the two processes. Experimentally, product ions resulting from N–C_α bond cleavage were on the order of 10 times more abundant than those from C_α–C bond cleavage,

dx.doi.org/10.1021/jp501367w | J. Phys. Chem. A 2014, 118, 8380–8392

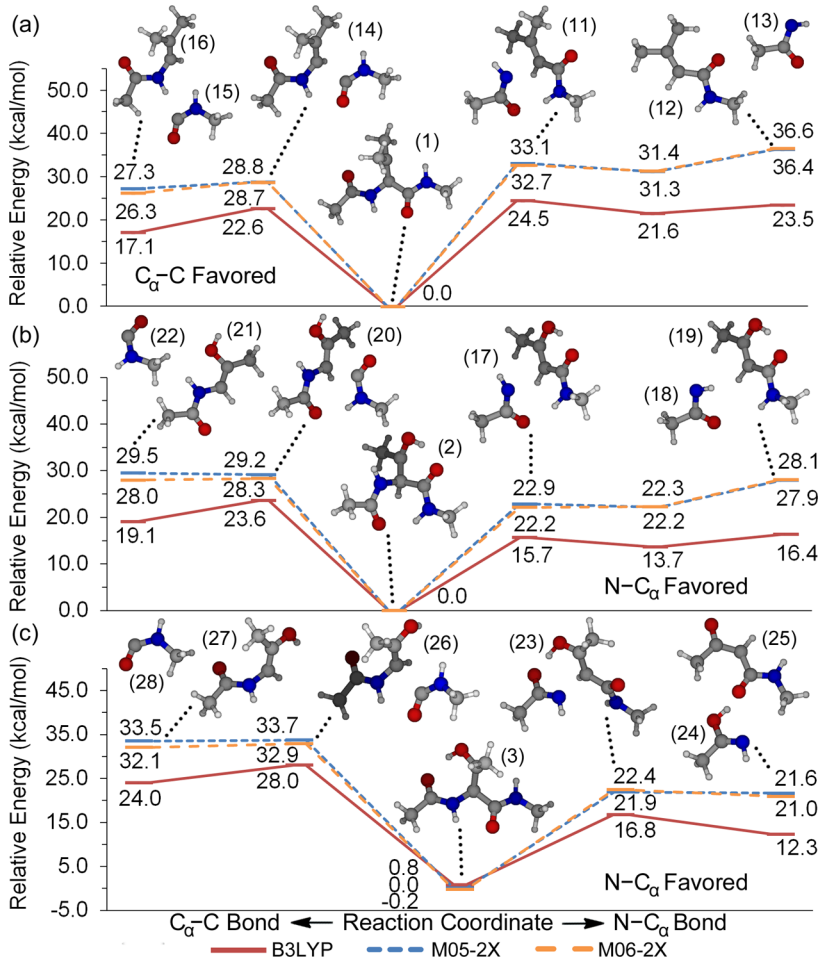

Figure 4. β-cleavage of the N–C_α vs C_α–C bond from a C_β-centered radical on model amino acids. For the valine model compound (a), dissociation of the C_α–C bond is favored, whereas hydrogen bonding in threonine (b and c) favors N–C_α bond cleavage via stabilization of the reaction intermediate. Enthalpies are given relative to structure **1** for the valine molecule and structure **2** for the threonine molecule.

meaning a significant difference in the reaction rates would be expected on the ion trap time scale. Previous work has demonstrated that even small differences in activation energy can have large impacts on the kinetics and branching ratios of peptide dissociation,[94,95] and dissociation of the N–C_α bond need only be slightly enthalpically favored to be the dominant product ion (assuming similar frequency factors for the two processes).

For the N-terminal hydrogen bonding structure (**3**) shown in Figure 4c, the preference for dissociation of the N–C_α bond over the C_α–C bond is quite clear. In this conformation, the energy required for cleavage of the N–C_α bond is significantly reduced due to the approach of the hydroxyl and carbonyl groups at the transition state (**23**) and subsequent hydrogen atom transfer to give the enol-imine (**24**) and carbon-centered radical (**25**) products (c and $[z - H]^\bullet$ ion analogues of Scheme 3b, respectively). The reaction coordinate for C_α–C bond cleavage shows that the threonine side chain rotates during dissociation, disrupting hydrogen bonding at the transition state (**26**) and forming the N-terminal product (**27**) with the hydroxyl group oriented outward along the axis of the N–C_α bond. This N-terminal product (a ion analogue) may readily isomerize to give the lower-energy structure seen in Figure 4b (**21**) and thereby reduce the reaction enthalpy, but the process still remains unfavorable due to the significant activation energy required to reach the transition state (**26**). Similar energetics with slightly higher barriers for all processes were found for a model serine compound (Figure S5, Supporting Information). Thus, the calculations outlined support both the data and proposed mechanism in concluding that hydrogen bond constraints favor N–C_α bond cleavage at serine and threonine residues.

Nitrogen-Centered Radical Chemistry via Loss of H_2O. The processes examined above fail to explain the presence of $x_m - H_2O$ and $a_n - H_2O$ ions. Therefore, calculations were also utilized to investigate the energetics of the mechanism shown in Scheme 3c, in which dissociation occurs through β-cleavage from a nitrogen-centered radical initially formed by water loss. The low-energy structures of the C_α-centered radical for the threonine and *O*-methylthreonine model compounds are shown in Figure 3c,e, respectively. For both model compounds, the low-energy structures (**4** and **7**) do not possess interactions between the side-chain hydroxyl and the N-terminal amide nitrogen that would give a clear pathway to the neutral loss of water, though such structures can be found for threonine (**5**) and *O*-methylthreonine (**8**) at relative enthalpies of 2.9 and 3.6 kcal/mol, respectively. In these conformations, the side-chain oxygen acts as hydrogen bond acceptor, with the backbone N–H group functioning as hydrogen bond donor. Water loss was found to occur from these structures via concerted cleavage of the side-chain C_β–OH bond and abstraction of hydrogen from the amide nitrogen, as shown in Figure 5a,b. This process

dx.doi.org/10.1021/jp501367w | J. Phys. Chem. A 2014, 118, 8380–8392

occurs via a tight transition state of 32−36 kcal/mol for both molecules, although the overall enthalpy of reaction in each case was favorable (10−20 kcal/mol).

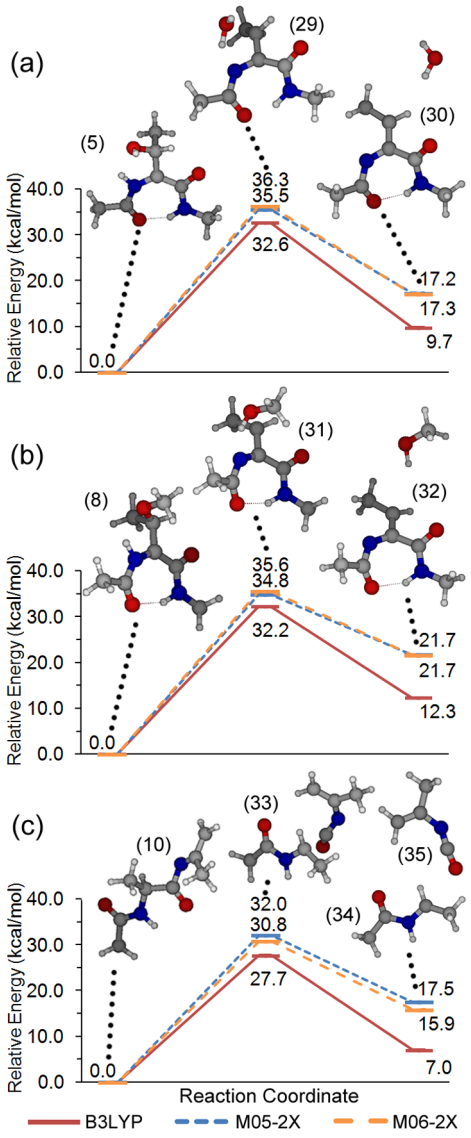

Figure 5. Energetics of alternate pathways to cleavage of the N-terminal C_α−C bond via formation of a nitrogen-centered radical: (a) water loss from threonine model compound; (b) methanol loss from *O*-methylthreonine model compound; (c) cleavage of C_α−C bond from nitrogen-centered radical. These processes have low reaction enthalpies but possess high activation energies.

Beginning from either threonine or *O*-methylthreonine, loss of water or methanol yields a nitrogen-centered radical and double bond between C_α and C_β (structures **30** and **32**, respectively). The structure shown in Figure 3g seeks to replicate these features in a model system to study the energetics of β-cleavage of the C_α−C bond. As illustrated in Figure 5c, cleavage of the C_α−C bond from the low-energy structure (**10**) was found to occur with a tight transition state but favorable reaction enthalpy as the N−C−O bond angle changes from 123° to 174° during formation of the double bond.

This pathway to dissociation of the C_α−C bond is essential to explain the experimental results for the *O*-methylthreonine model peptide (Figure 1c). Methylation of the hydroxyl group prevents any conformation in which the side chain acts as hydrogen bond donor, thereby suggesting that the two mechanisms presented in Scheme 3a,b are inoperable for this molecule. In agreement with this assertion, it was found that cleavage of the N−C_α bond via β-cleavage from the low-energy C_β-centered radical structure (**6**, Figure 3d) was not energetically favorable (Figure S6, Supporting Information). However, β-cleavage from a nitrogen-centered radical in *O*-methylthreonine residues gives a viable route to the observed $[a_{n-1} + H]^\bullet$ ion even in the absence of a side-chain hydrogen bond donor. In addition, the energetics for this process are only slightly higher than those calculated for C_α−C bond cleavage, further supporting the feasibility of this pathway.

In the case of the threonine model compound possessing a free hydroxyl group, there exists a significant disparity between the experimental observation of the water loss pathway outlined in Scheme 3c and the theoretical activation energies for this reaction. The theoretical barrier to water loss of 32−36 kcal/mol is 7−14 kcal/mol higher than those calculated for the processes outlined in Scheme 3a,b and therefore would not be expected to compete. Because the experimental data provide compelling evidence for the proposed reaction pathway leading to water loss, especially the MS^4 spectra shown in Figure 2, it appears that these calculations overestimate the activation energy for this pathway. A conformation with a lower barrier to water loss may exist, but extensive conformational searching failed to yield a transition state lower in energy than the one shown in Figure 5a. Alternately, the activation energy for this process may be lowered by cleavage of the backbone C_α−C bond in concert with hydrogen atom transfer from the amide to the hydroxyl group, a process somewhat analogous to that proposed in Scheme 3b. A concerted reaction would also explain the low abundance of water loss in the FRIPS spectra, but such processes were not examined using DFT calculations due to the difficulty in searching the expanded conformational space to identify the minimum energy pathway.

Why Hydrogen Bonding Favors N−C_α Bond Cleavage. Although calculations can quantify the energetics of the proposed processes leading to cleavage of the stronger N−C_α bond in the mechanisms shown in Scheme 3a,b, it is useful to provide a simpler but more transposable rationalization for why these reactions occur by examining the molecular orbitals involved. Strong orbital overlap connecting reactants to products is generally associated with favorable chemical reactions, whereas little overlap leads to energetically unfavorable processes.[96] Parts a and b of Figure 6 show schematically the interaction between the singly occupied π orbital of the C_β-radical site and the N−C_α σ bond for the N-terminal hydrogen bonding and C-terminal hydrogen bonding complexes, respectively. In either structure, the hydrogen bonding interactions strongly align the π orbital on C_β with the N−C_α σ bond, resulting in facile cleavage of the N−C_α bond. In contrast, the C_α−C σ bond lies nearly orthogonal to the π orbital on C_β in both conformations, and the cleavage of this bond is therefore unfavorable without the destruction of the stabilizing hydrogen bonding interactions.

In addition to orbital overlap, the transition state structures for both conformations are stabilized by enhanced hydrogen bonding. This observation is illustrated in Scheme 4, which gives the bond lengths in Angstroms for the N-terminal (a) and C-terminal (b) hydrogen bonding conformations in both the ground state (GS) and transition state (TS). In the C-terminal

dx.doi.org/10.1021/jp501367w | J. Phys. Chem. A 2014, 118, 8380−8392

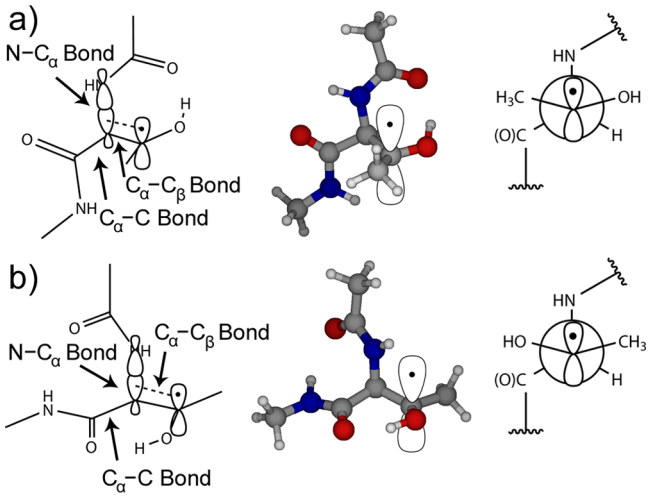

Figure 6. Alignment of the singly occupied π orbital on C_β with the N–C_α σ bond via hydrogen bonding interactions of threonine with either the N-terminal (a) or C-terminal (b) carbonyl oxygen. Left: schematic representation of computational structures, with orbital alignment denoted by the dashed line. Center: computational structures with schematic representation of the singly occupied π orbital on C_β. Right: Newman projection along the axis of the C_β–C_α bond.

Scheme 4. Calculated Bond Lengths (Å) during N–C_α Bond Cleavage for the Threonine Model Compound Possessing an (a) N-Terminal or (b) C-Terminal Hydrogen Bond

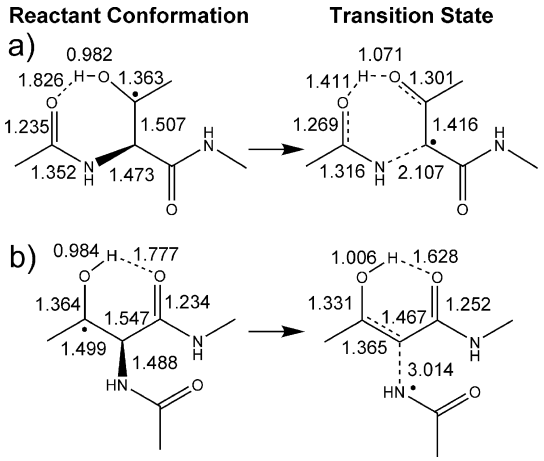

hydrogen bonding structure, the distance between the carbonyl oxygen and the hydroxyl group hydrogen decreases from 1.78 Å in the ground state to 1.63 Å in the transition state, imparting a stabilizing partial double bond character to the hydroxyl group. In the case of the N-terminal hydrogen bonding conformer, the hydrogen atom approaches to a distance of only 1.4 Å from the carbonyl at the transition state for N–C_α bond cleavage, forming a stabilizing intermediate with increased bond order on the side-chain C_β–O bond. These hydrogen bonding interactions therefore play a crucial role in dictating the favored pathway of the reaction.

Comparison of FRIPS to ECD/ETD. The process of hydrogen atom transfer along with N–C_α bond cleavage (Scheme 3b) examined in this work gives product ions with remarkable resemblance to those observed in ECD and ETD. In the UW mechanism, which is supported by numerous experimental and theoretical reports, an aminoketyl intermediate may be formed either through direct electron capture to the amide π^* orbital or through intramolecular electron transfer from electron capture in a Rydberg orbital at a positively charged site, followed by proton abstraction by the strongly basic amide anion radical.[19,29−31,39] The mechanism proposed here is more comparable to the Cornell mechanism, in which hydrogen atom transfer is suggested to form the aminoketyl intermediate, with backbone cleavage occurring separately.[19,32,33,37] However, the proposed mechanism for radical-induced cleavage at serine and threonine is absent of any aminoketyl intermediate, as the transfer of the hydrogen atom occurs in concert with N–C_α bond cleavage. Further examination of the potential energy surface failed to find a pathway in which aminoketyl intermediate formation was more energetically favorable than concerted hydrogen atom transfer and N–C_α bond cleavage, making this dissociation mechanism unlikely for this system. In addition, the Cornell mechanism is unlikely to be prevalent in ECD and ETD, as the energetic barriers to hydrogen atom transfer are greater than those to intramolecular electron transfer followed by proton abstraction.[19,24] Although not directly applicable to the ECD or ETD case, the hydrogen atom transfer observed here is interesting in that it illuminates yet another unique mechanism for the cleavage of backbone N–C_α bonds via a decrease in the energetic requirements for this process.

CONCLUSIONS

The calculations and experiments detailed in this work provide a comprehensive analysis of the factors responsible for the unique free radical chemistry of serine and threonine. Cleavage of the N–C_α bond may occur directly via β-cleavage from a C_β-centered radical, whereas dissociation of the N-terminal C_α–C bond may occur either from a nitrogen-centered radical or by loss of isocyanic acid following N–C_α bond cleavage. As a result of the lower energetic barriers associated with odd-electron versus even-electron cleavage processes, these reaction pathways are more susceptible to influence by weak interactions such as hydrogen bonding that constrain molecular geometry in reactants, intermediates, and products. This principle has significant implications for gas-phase free radical sequencing applications, in which many peptides and proteins may possess stable gas-phase noncovalent interactions that may direct radical-induced dissociation, an attribute that Julian and co-workers have leveraged to elucidate the gas phase structure of proteins.[58,60,77] In other situations, such effects may be masked by rapid migration of the radical site following formation.[79] Nevertheless, it is abundantly clear from this work that free radical chemistry can be highly sensitive to local conformation at the radical site, as no fewer than five unique dissociation pathways can occur at serine and threonine residues via dissociation from different conformations.

ASSOCIATED CONTENT

Supporting Information

Additional MS^n data, theoretical calculations, synthesis details, reaction energetics, geometries, energies, and partial charges of theoretical structures. This material is available free of charge via the Internet at http://pubs.acs.org.

AUTHOR INFORMATION

Corresponding Author

*J. L. Beauchamp: phone, 626-395-6525; fax, 626-395-4912; e-mail, jlbchamp@caltech.edu.

Notes

The authors declare no competing financial interest.

■ ACKNOWLEDGMENTS

The authors acknowledge Wei-Guang Liu and Prof. William A. Goddard III for their assistance and instruction in the use of software used to perform theoretical calculations as well as the Materials and Process Simulation Center at Caltech, which kindly provided computational resources. This project was funded and supported by the Beckman Institute at Caltech and in its early stages by National Science Foundation grant CHE-0416381.

■ REFERENCES

(1) Bogdanov, B.; Smith, R. D. Proteomics by FTICR Mass Spectrometry: Top Down and Bottom Up. *Mass Spectrom. Rev.* **2005**, *24*, 168−200.
(2) Petrotchenko, E. V.; Borchers, C. H. Crosslinking Combined with Mass Spectrometry for Structural Proteomics. *Mass Spectrom. Rev.* **2010**, *29*, 862−876.
(3) Lee, J.; Soper, S. A.; Murray, K. K. Microfluidic Chips for Mass Spectrometry-Based Proteomics. *J. Mass Spectrom.* **2009**, *44*, 579−593.
(4) Cooper, H. J.; Håkansson, K.; Marshall, A. G. The Role of Electron Capture Dissociation in Biomolecular Analysis. *Mass Spectrom. Rev.* **2005**, *24*, 201−222.
(5) Shen, Y.; Zhao, R.; Berger, S. J.; Anderson, G. A.; Rodriguez, N.; Smith, R. D. High-Efficiency Nanoscale Liquid Chromatography Coupled On-Line with Mass Spectrometry Using Nanoelectrospray Ionization for Proteomics. *Anal. Chem.* **2002**, *74*, 4235−4249.
(6) Senko, M. W.; Speir, J. P.; McLafferty, F. W. Collisional Activation of Large Multiply Charged Ions Using Fourier Transform Mass Spectrometry. *Anal. Chem.* **1994**, *66*, 2801−2808.
(7) Little, D. P.; Speir, J. P.; Senko, M. W.; O'Connor, P. B.; McLafferty, F. W. Infrared Multiphoton Dissociation of Large Multiply Charged Ions for Biomolecule Sequencing. *Anal. Chem.* **1994**, *66*, 2809−2815.
(8) Kruger, N. A.; Zubarev, R. A.; Carpenter, B. K.; Kelleher, N. L.; Horn, D. M.; McLafferty, F. W. Electron Capture versus Energetic Dissociation of Protein Ions. *Int. J. Mass Spectrom.* **1999**, *182*−*183*, 1−5.
(9) Håkansson, K.; Cooper, H. J.; Emmett, M. R.; Costello, C. E.; Marshall, A. G.; Nilsson, C. L. Electron Capture Dissociation and Infrared Multiphoton Dissociation MS/MS of an N-Glycosylated Tryptic Peptide To Yield Complementary Sequence Information. *Anal. Chem.* **2001**, *73*, 4530−4536.
(10) Shukla, A. K.; Futrell, J. H. Tandem Mass Spectrometry: Dissociation of Ions by Collisional Activation. *J. Mass Spectrom.* **2000**, *35*, 1069−1090.
(11) Paizs, B.; Suhai, S. Fragmentation Pathways of Protonated Peptides. *Mass Spectrom. Rev.* **2005**, *24*, 508−548.
(12) Tureček, F.; Julian, R. R. Peptide Radicals and Cation Radicals in the Gas Phase. *Chem. Rev.* **2013**, *113*, 6691−6733.
(13) Zubarev, R. A.; Kelleher, N. L.; McLafferty, F. W. Electron Capture Dissociation of Multiply Charged Protein Cations. A Nonergodic Process. *J. Am. Chem. Soc.* **1998**, *120*, 3265−3266.
(14) Kruger, N. A.; Zubarev, R. A.; Horn, D. M.; McLafferty, F. W. Electron Capture Dissociation of Multiply Charged Peptide Cations. *Int. J. Mass Spectrom.* **1999**, *185*−*187*, 787−793.
(15) Syka, J. E. P.; Coon, J. J.; Schroeder, M. J.; Shabanowitz, J.; Hunt, D. F. Peptide and Protein Sequence Analysis by Electron Transfer Dissociation Mass Spectrometry. *Proc. Natl. Acad. Sci. U. S. A.* **2004**, *101*, 9528−9533.
(16) Zubarev, R. A.; Kruger, N. A.; Fridriksson, E. K.; Lewis, M. A.; Horn, D. M.; Carpenter, B. K.; McLafferty, F. W. Electron Capture Dissociation of Gaseous Multiply-Charged Proteins Is Favored at Disulfide Bonds and Other Sites of High Hydrogen Atom Affinity. *J. Am. Chem. Soc.* **1999**, *121*, 2857−2862.
(17) Zubarev, R. A.; Horn, D. M.; Fridriksson, E. K.; Kelleher, N. L.; Kruger, N. A.; Lewis, M. A.; Carpenter, B. K.; McLafferty, F. W. Electron Capture Dissociation for Structural Characterization of Multiply Charged Protein Cations. *Anal. Chem.* **2000**, *72*, 563−573.
(18) Zubarev, R. A.; Haselmann, K. F.; Budnik, B.; Kjeldsen, F.; Jensen, F. Account: Towards an Understanding of the Mechanism of Electron-Capture Dissociation: A Historical Perspective and Modern Ideas. *Eur. J. Mass Spectrom.* **2002**, *8*, 337−349.
(19) Simons, J. Mechanisms for S-S and N-C_α Bond Cleavage in Peptide ECD and ETD Mass Spectrometry. *Chem. Phys. Lett.* **2010**, *484*, 81−95.
(20) Iavarone, A. T.; Paech, K.; Williams, E. R. Effects of Charge State and Cationizing Agent on the Electron Capture Dissociation of a Peptide. *Anal. Chem.* **2004**, *76*, 2231−2238.
(21) Chamot-Rooke, J.; Malosse, C.; Frison, G.; Tureček, F. Electron Capture in Charge-Tagged Peptides. Evidence for the Role of Excited Electronic States. *J. Am. Soc. Mass Spectrom.* **2007**, *18*, 2146−2161.
(22) Xia, Y.; Gunawardena, H. P.; Erickson, D. E.; McLuckey, S. A. Effects of Cation Charge-Site Identity and Position on Electron-Transfer Dissociation of Polypeptide Cations. *J. Am. Chem. Soc.* **2007**, *129*, 12232−12243.
(23) Anusiewicz, I.; Berdys-Kochanska, J.; Simons, J. Electron Attachment Step in Electron Capture Dissociation (ECD) and Electron Transfer Dissociation (ETD). *J. Phys. Chem. A* **2005**, *109*, 5801−5813.
(24) Anusiewicz, I.; Berdys-Kochanska, J.; Skurski, P.; Simons, J. Simulating Electron Transfer Attachment to a Positively Charged Model Peptide. *J. Phys. Chem. A* **2006**, *110*, 1261−1266.
(25) Sawicka, A.; Skurski, P.; Hudgins, R. R.; Simons, J. Model Calculations Relevant to Disulfide Bond Cleavage via Electron Capture Influenced by Positively Charged Groups. *J. Phys. Chem. B* **2003**, *107*, 13505−13511.
(26) Sawicka, A.; Berdys-Kochańska, J.; Skurski, P.; Simons, J. Low-Energy (0.1 eV) Electron Attachment S-S Bond Cleavage Assisted by Coulomb Stabilization. *Int. J. Quantum Chem.* **2005**, *102*, 838−846.
(27) Sobczyk, M.; Anusiewicz, I.; Berdys-Kochanska, J.; Sawicka, A.; Skurski, P.; Simons, J. Coulomb-Assisted Dissociative Electron Attachment: Application to a Model Peptide. *J. Phys. Chem. A* **2005**, *109*, 250−258.
(28) Skurski, P.; Sobczyk, M.; Jakowski, J.; Simons, J. Possible Mechanisms for Protecting N-C_α Bonds in Helical Peptides from Electron-Capture (or Transfer) Dissociation. *Int. J. Mass Spectrom.* **2007**, *265*, 197−212.
(29) Sobczyk, M.; Simons, J. Distance Dependence of Through-Bond Electron Transfer Rates in Electron-Capture and Electron-Transfer Dissociation. *Int. J. Mass Spectrom.* **2006**, *253*, 274−280.
(30) Sobczyk, M.; Simons, J. The Role of Excited Rydberg States in Electron Transfer Dissociation. *J. Phys. Chem. B* **2006**, *110*, 7519−7527.
(31) Sobczyk, M.; Neff, D.; Simons, J. Theoretical Study of Through-Space and Through-Bond Electron Transfer within Positively Charged Peptides in the Gas Phase. *Int. J. Mass Spectrom.* **2008**, *269*, 149−164.
(32) Tureček, F. N-C_α Bond Dissociation Energies and Kinetics in Amide and Peptide Radicals. Is the Dissociation a Non-ergodic Process? *J. Am. Chem. Soc.* **2003**, *125*, 5954−5963.
(33) Syrstad, E.; Tureček, F. Toward a general mechanism of electron capture dissociation. *J. Am. Soc. Mass Spectrom.* **2005**, *16*, 208−224.
(34) Tureček, F.; Chen, X.; Hao, C. Where Does the Electron Go? Electron Distribution and Reactivity of Peptide Cation Radicals Formed by Electron Transfer in the Gas phase. *J. Am. Chem. Soc.* **2008**, *130*, 8818−8833.
(35) Chen, X.; Tureček, F. The Arginine Anomaly: Arginine Radicals Are Poor Hydrogen Atom Donors in Electron Transfer Induced Dissociations. *J. Am. Chem. Soc.* **2006**, *128*, 12520−12530.
(36) Syrstad, E. A.; Tureček, F. Hydrogen Atom Adducts to the Amide Bond. Generation and Energetics of the Amino(hydroxy)-methyl Radical in the Gas Phase. *J. Phys. Chem. A* **2001**, *105*, 11144−11155.

(37) Tureček, F.; Syrstad, E. A. Mechanism and Energetics of Intramolecular Hydrogen Transfer in Amide and Peptide Radicals and Cation-Radicals. *J. Am. Chem. Soc.* **2003**, *125*, 3353−3369.
(38) Syrstad, E. A.; Stephens, D. D.; Tureček, F. Hydrogen Atom Adducts to the Amide Bond. Generation and Energetics of Amide Radicals in the Gas Phase. *J. Phys. Chem. A* **2003**, *107*, 115−126.
(39) Sohn, C. H.; Chung, C. K.; Yin, S.; Ramachandran, P.; Loo, J. A.; Beauchamp, J. L. Probing the Mechanism of Electron Capture and Electron Transfer Dissociation Using Tags with Variable Electron Affinity. *J. Am. Chem. Soc.* **2009**, *131*, 5444−5459.
(40) Frison, G.; van der Rest, G.; Tureček, F.; Besson, T.; Lemaire, J. l.; Maître, P.; Chamot-Rooke, J. Structure of Electron-Capture Dissociation Fragments from Charge-Tagged Peptides Probed by Tunable Infrared Multiple Photon Dissociation. *J. Am. Chem. Soc.* **2008**, *130*, 14916−14917.
(41) Tureček, F. Electron Predators are Hydrogen Atom Traps. Effects of Aryl Groups on N−C_α Bond Dissociations of Peptide Radicals. *J. Mass Spectrom.* **2010**, *45*, 1280−1290.
(42) Bakhtiar, R.; Guan, Z. Electron Capture Dissociation Mass Spectrometry in Characterization of Post-Translational Modifications. *Biochem. Biophys. Res. Commun.* **2005**, *334*, 1−8.
(43) Siuti, N.; Kelleher, N. L. Decoding Protein Modifications Using Top-Down Mass Spectrometry. *Nat. Methods* **2007**, *4*, 817−821.
(44) Shi, S. D. H.; Hemling, M. E.; Carr, S. A.; Horn, D. M.; Lindh, I.; McLafferty, F. W. Phosphopeptide/Phosphoprotein Mapping by Electron Capture Dissociation Mass Spectrometry. *Anal. Chem.* **2000**, *73*, 19−22.
(45) Adamson, J. T.; Håkansson, K. Infrared Multiphoton Dissociation and Electron Capture Dissociation of High-Mannose Type Glycopeptides. *J. Proteome Res.* **2006**, *5*, 493−501.
(46) Simon, M. D.; Chu, F.; Racki, L. R.; de la Cruz, C. C.; Burlingame, A. L.; Panning, B.; Narlikar, G. J.; Shokat, K. M. The Site-Specific Installation of Methyl-Lysine Analogs into Recombinant Histones. *Cell* **2007**, *128*, 1003−1012.
(47) Hopkinson, A. C. Radical Cations of Amino Acids and Peptides: Structures and Stabilities. *Mass Spectrom. Rev.* **2009**, *28*, 655−671.
(48) Chu, I. K.; Rodriquez, C. F.; Lau, T.-C.; Hopkinson, A. C.; Siu, K. W. M. Molecular Radical Cations of Oligopeptides. *J. Phys. Chem. B* **2000**, *104*, 3393−3397.
(49) Wee, S.; O'Hair, R. A. J.; McFadyen, W. D. Comparing the Gas-Phase Fragmentation Reactions of Protonated and Radical Cations of the Tripeptides GXR. *Int. J. Mass Spectrom.* **2004**, *234*, 101−122.
(50) Bagheri-Majdi, E.; Ke, Y.; Orlova, G.; Chu, I. K.; Hopkinson, A. C.; Siu, K. W. M. Copper-Mediated Peptide Radical Ions in the Gas Phase. *J. Phys. Chem. B* **2004**, *108*, 11170−11181.
(51) Barlow, C. K.; Wee, S.; McFadyen, W. D.; x; Hair, R. A. J. Designing Copper(II) Ternary Complexes to Generate Radical Cations of Peptides in the Gas Phase: Role of the Auxiliary Ligand. *Dalton Trans.* **2004**, 3199−3204.
(52) Ke, Y.; Zhao, J.; Verkerk, U. H.; Hopkinson, A. C.; Siu, K. W. M. Histidine, Lysine, and Arginine Radical Cations: Isomer Control via the Choice of Auxiliary Ligand (L) in the Dissociation of $[Cu^{II}(L)(\text{amino acid})]^{\bullet 2+}$ Complexes. *J. Phys. Chem. B* **2007**, *111*, 14318−14328.
(53) Laskin, J.; Yang, Z.; Chu, I. K. Energetics and Dynamics of Electron Transfer and Proton Transfer in Dissociation of $Metal^{III}$(salen)−Peptide Complexes in the Gas Phase. *J. Am. Chem. Soc.* **2008**, *130*, 3218−3230.
(54) Wee, S.; O'Hair, R. A. J.; McFadyen, W. D. The Role of the Position of the Basic Residue in the Generation and Fragmentation of Peptide Radical Cations. *Int. J. Mass Spectrom.* **2006**, *249*−*250*, 171−183.
(55) Thompson, M. S.; Cui, W.; Reilly, J. P. Fragmentation of Singly Charged Peptide Ions by Photodissociation at λ=157 nm. *Angew. Chem., Int. Ed.* **2004**, *43*, 4791−4794.
(56) Cui, W.; Thompson, M. S.; Reilly, J. P. Pathways of Peptide Ion Fragmentation Induced by Vacuum Ultraviolet Light. *J. Am. Soc. Mass Spectrom.* **2005**, *16*, 1384−1398.
(57) Kim, T.-Y.; Thompson, M. S.; Reilly, J. P. Peptide Photodissociation at 157 nm in a Linear Ion Trap Mass Spectrometer. *Rapid Commun. Mass Spectrom.* **2005**, *19*, 1657−1665.
(58) Ly, T.; Julian, R. R. Residue-Specific Radical-Directed Dissociation of Whole Proteins in the Gas Phase. *J. Am. Chem. Soc.* **2007**, *130*, 351−358.
(59) Sun, Q.; Yin, S.; Loo, J. A.; Julian, R. R. Radical Directed Dissociation for Facile Identification of Iodotyrosine Residues Using Electrospray Ionization Mass Spectrometry. *Anal. Chem.* **2010**, *82*, 3826−3833.
(60) Ly, T.; Julian, R. R. Elucidating the Tertiary Structure of Protein Ions in Vacuo with Site Specific Photoinitiated Radical Reactions. *J. Am. Chem. Soc.* **2010**, *132*, 8602−8609.
(61) Masterson, D. S.; Yin, H.; Chacon, A.; Hachey, D. L.; Norris, J. L.; Porter, N. A. Lysine Peroxycarbamates: Free Radical-Promoted Peptide Cleavage. *J. Am. Chem. Soc.* **2003**, *126*, 720−721.
(62) Yin, H.; Chacon, A.; Porter, N. A.; Masterson, D. S. Free Radical-Induced Site-Specific Peptide Cleavage in the Gas Phase: Low-Energy Collision-Induced Dissociation in ESI- and MALDI Mass Spectrometry. *J. Am. Soc. Mass Spectrom.* **2007**, *18*, 807−816.
(63) Ryzhov, V.; Lam, A.; O'Hair, R. Gas-Phase Fragmentation of Long-Lived Cysteine Radical Cations formed via NO Loss from Protonated S-Nitrosocysteine. *J. Am. Soc. Mass Spectrom.* **2009**, *20*, 985−995.
(64) Wee, S.; Mortimer, A.; Moran, D.; Wright, A.; Barlow, C. K.; O'Hair, R. A. J.; Radom, L.; Easton, C. J. Gas-Phase Regiocontrolled Generation of Charged Amino Acid and Peptide Radicals. *Chem. Commun.* **2006**, 4233−4235.
(65) Lam, A. K. Y.; Ryzhov, V.; O'Hair, R. A. J. Mobile Protons versus Mobile Radicals: Gas-Phase Unimolecular Chemistry of Radical Cations of Cysteine-Containing Peptides. *J. Am. Soc. Mass Spectrom.* **2010**, *21*, 1296−1312.
(66) Barlow, C. K.; Wright, A.; Easton, C. J.; O'Hair, R. A. J. Gas-Phase Ion−Molecule Reactions Using Regioselectively Generated Radical Cations To Model Oxidative Damage and Probe Radical Sites in Peptides. *Org. Biomol. Chem.* **2011**, *9*, 3733−3745.
(67) Osburn, S.; O'Hair, R. A. J.; Ryzhov, V. Gas-Phase Reactivity of Sulfur-Based Radical Ions of Cysteine Derivatives and Small Peptides. *Int. J. Mass Spectrom.* **2012**, *316*-*318*, 133−139.
(68) Hodyss, R.; Cox, H. A.; Beauchamp, J. L. Bioconjugates for Tunable Peptide Fragmentation: Free Radical Initiated Peptide Sequencing (FRIPS). *J. Am. Chem. Soc.* **2005**, *127*, 12436−12437.
(69) Lee, M.; Kang, M.; Moon, B.; Oh, H. B. Gas-phase Peptide Sequencing by TEMPO-Mediated Radical Generation. *Analyst* **2009**, *134*, 1706−1712.
(70) Sohn, C. H. New Reagents and Methods for Mass Spectrometry-Based Proteomics Investigations. *Ph.D. Dissertation*, California Institute of Technology, Pasadena, CA, 2011. http://resolver.caltech.edu/CaltechTHESIS:02162011-180032183
(71) Lee, M.; Lee, Y.; Kang, M.; Park, H.; Seong, Y.; June Sung, B.; Moon, B.; Bin Oh, H. Disulfide Bond Cleavage in TEMPO-Free Radical Initiated Peptide Sequencing Mass Spectrometry. *J. Mass Spectrom.* **2011**, *46*, 830−839.
(72) Lee, J.; Park, H.; Kwon, H.; Kwon, G.; Jeon, A.; Kim, H. I.; Sung, B. J.; Moon, B.; Oh, H. B. One-Step Peptide Backbone Dissociations in Negative-Ion Free Radical Initiated Peptide Sequencing Mass Spectrometry. *Anal. Chem.* **2013**, *85*, 7044−7051.
(73) Laskin, J.; Yang, Z.; Ng, C. M. D.; Chu, I. K. Fragmentation of Alpha-Radical Cations of Arginine-Containing Peptides. *J. Am. Soc. Mass Spectrom.* **2010**, *21*, 511−521.
(74) Laskin, J.; Yang, Z.; Lam, C.; Chu, I. K. Charge-Remote Fragmentation of Odd-Electron Peptide Ions. *Anal. Chem.* **2007**, *79*, 6607−6614.
(75) Sun, Q.; Nelson, H.; Ly, T.; Stoltz, B. M.; Julian, R. R. Side Chain Chemistry Mediates Backbone Fragmentation in Hydrogen Deficient Peptide Radicals. *J. Proteome Res.* **2008**, *8*, 958−966.
(76) Moore, B.; Sun, Q.; Hsu, J.; Lee, A.; Yoo, G.; Ly, T.; Julian, R. Dissociation Chemistry of Hydrogen-Deficient Radical Peptide Anions. *J. Am. Soc. Mass Spectrom.* **2012**, *23*, 460−468.

(77) Zhang, X.; Julian, R. R. Investigating the Gas Phase Structure of KIX with Radical Directed Dissociation and Molecular Dynamics: Retention of the Native Structure. *Int. J. Mass Spectrom.* **2011**, *308*, 225−231.
(78) Zhang, X.; Julian, R. R. Exploring Radical Migration Pathways in Peptides with Positional Isomers, Deuterium Labeling, and Molecular Dynamics Simulations. *J. Am. Soc. Mass Spectrom.* **2013**, *24*, 524−533.
(79) Moore, B. N.; Blanksby, S. J.; Julian, R. R. Ion−Molecule Reactions Reveal Facile Radical Migration in Peptides. *Chem. Commun.* **2009**, 5015−5017.
(80) Ly, T.; Julian, R. R. Tracking Radical Migration in Large Hydrogen Deficient Peptides with Covalent Labels: Facile Movement Does Not Equal Indiscriminate Fragmentation. *J. Am. Soc. Mass Spectrom.* **2009**, *20*, 1148−1158.
(81) Diedrich, J. K.; Julian, R. R. Facile Identification of Phosphorylation Sites in Peptides by Radical Directed Dissociation. *Anal. Chem.* **2011**, *83*, 6818−6826.
(82) Diedrich, J. K.; Julian, R. R. Site-Selective Fragmentation of Peptides and Proteins at Quinone-Modified Cysteine Residues Investigated by ESI-MS. *Anal. Chem.* **2010**, *82*, 4006−4014.
(83) Tao, Y.; Quebbemann, N. R.; Julian, R. R. Discriminating d-Amino Acid-Containing Peptide Epimers by Radical-Directed Dissociation Mass Spectrometry. *Anal. Chem.* **2012**, *84*, 6814−6820.
(84) Zhang, L.; Reilly, J. P. Radical-Driven Dissociation of Odd-Electron Peptide Radical Ions Produced in 157 nm Photodissociation. *J. Am. Soc. Mass Spectrom.* **2009**, *20*, 1378−1390.
(85) Schaftenaar, G.; Noordik, J. H. Molden: a Pre- and Post-processing Program for Molecular and Electronic Structures. *J. Comput.-Aided Mol. Des.* **2000**, *14*, 123−134.
(86) Zhao, Y.; Schultz, N. E.; Truhlar, D. G. Design of Density Functionals by Combining the Method of Constraint Satisfaction with Parametrization for Thermochemistry, Thermochemical Kinetics, and Noncovalent Interactions. *J. Chem. Theory Comput.* **2006**, *2*, 364−382.
(87) Zhao, Y.; Truhlar, D. The M06 Suite of Density Functionals for Main Group Thermochemistry, Thermochemical Kinetics, Noncovalent Interactions, Excited States, and Transition Elements: Two New Functionals and Systematic Testing of Four M06-class Functionals and 12 Other Functionals. *Theor. Chem. Acc.* **2008**, *120*, 215−241.
(88) Zhao, Y.; Truhlar, D. G. How Well Can New-Generation Density Functionals Describe the Energetics of Bond-Dissociation Reactions Producing Radicals? *J. Phys. Chem. A* **2008**, *112*, 1095−1099.
(89) Gronert, S.; O'Hair, R. A. J. Ab Initio Studies of Amino Acid Conformations. 1. The Conformers of Alanine, Serine, and Cysteine. *J. Am. Chem. Soc.* **1995**, *117*, 2071−2081.
(90) Fu, A.-p.; Du, D.-m.; Zhou, Z.-y. Density Functional Theory Study of the Hydrogen Bonding Interaction of 1:1 Complexes of Formamide with Methanol. *Chem. Phys. Lett.* **2003**, *377*, 537−543.
(91) Miao, R.; Jin, C.; Yang, G.; Hong, J.; Zhao, C.; Zhu, L. Comprehensive Density Functional Theory Study on Serine and Related Ions in Gas Phase: Conformations, Gas Phase Basicities, and Acidities. *J. Phys. Chem. A* **2005**, *109*, 2340−2349.
(92) Wendler, K.; Thar, J.; Zahn, S.; Kirchner, B. Estimating the Hydrogen Bond Energy. *J. Phys. Chem. A* **2010**, *114*, 9529−9536.
(93) Izgorodina, E. I.; Brittain, D. R. B.; Hodgson, J. L.; Krenske, E. H.; Lin, C. Y.; Namazian, M.; Coote, M. L. Should Contemporary Density Functional Theory Methods Be Used To Study the Thermodynamics of Radical Reactions? *J. Phys. Chem. A* **2007**, *111*, 10754−10768.
(94) Marzluff, E. M.; Beauchamp, J. L. Collisional Activation Studies of Large Molecules. *Large Ions: Their Vaporization, Detection, and Structural Analysis*; Wiley: Chichester, U.K., and New York, 1996; pp 115−143.
(95) Marzluff, E. M.; Campbell, S.; Rodgers, M. T.; Beauchamp, J. L. Low-Energy Dissociation Pathways of Small Deprotonated Peptides in the Gas Phase. *J. Am. Chem. Soc.* **1994**, *116*, 7787−7796.
(96) Anh, N. T. *Frontier Orbitals: A Practical Manual*, 1st ed.; John Wiley and Sons: Hoboken, NJ, 2007.